A novel curcumin derivative for the treatment of diabetic neuropathy

Daniel J. Daugherty[a,*], **Alexandra Marquez**[b], **Nigel A. Calcutt**[b], and **David Schubert**[a]

[a]The Salk Institute for Biological Studies, La Jolla, CA, USA

[b]Department of Pathology, UCSD, La Jolla, CA, USA

Abstract

Neuropathy is a common complication of long-term diabetes. Proposed mechanisms of neuronal damage caused by diabetes that are downstream of hyperglycemia and/or loss of insulin signaling include ischemic hypoxia, inflammation and loss of neurotrophic support. The curcumin derivative J147 is a potent neurogenic and neuroprotective drug candidate initially developed for the treatment of neurodegenerative conditions associated with aging that impacts many pathways implicated in the pathogenesis of diabetic neuropathy. Here, we demonstrate efficacy of J147 in ameliorating multiple indices of neuropathy in the streptozotocin-induced mouse model of type 1 diabetes. Diabetes was determined by blood glucose, HbA1c, and insulin levels and efficacy of J147 by behavioral, physiologic, biochemical, proteomic, and transcriptomic assays. Biological efficacy of systemic J147 treatment was confirmed by its capacity to decrease TNFα pathway activation and several other markers of neuroinflammation in the CNS. Chronic oral treatment with J147 protected the sciatic nerve from progressive diabetes-induced slowing of large myelinated fiber conduction velocity while single doses of J147 rapidly and transiently reversed established touch-evoked allodynia. Conduction slowing and allodynia are clinically relevant markers of early diabetic neuropathy and neuropathic pain, respectively. RNA expression profiling suggests that one of the pathways by which J147 imparts its protection against diabetic induced neuropathy may be through activation of the AMP kinase pathway. The diverse biological and therapeutic effects of J147 suggest it as an alternative to the polypharmaceutical approaches required to treat the multiple pathogenic mechanisms that contribute to diabetic neuropathy.

Keywords

Diabetes; Neuropathy; J147; Inflammation; AMP kinase

1. Introduction

Diabetic neuropathy disrupts the quality of life of over half of all people with type 1 and type 2 diabetes. There is no FDA-approved treatment for diabetic neuropathy and the only current recommendation for prevention and slowing of symptoms is the maintenance of glycemic control (Pop-Busui and Martin, 2016). Unfortunately, maintaining consistent

---

*Corresponding author: Schubert@salk.edu (D.J. Daugherty).

euglycemia is difficult for the majority of people suffering from diabetes. Preclinical studies have suggested that the pathogenesis of diabetic neuropathy may derive from both hyperglycemia and loss of neurotrophic support from insulin/C-peptide. Multiple downstream pathways have been identified, which creates both opportunity and challenges for developing therapies (Biessels et al., 2014; Yagihashi, 2016; Zochodne, 2016). The traditional approach has been to target one pathway to establish proof of concept and then demonstrate clinical efficacy. However, there is emerging recognition that polypharmacy may be required in order to target multiple pathogenic pathways (Davidson et al., 2015). It would therefore be most beneficial to develop a therapy that impacts multiple pathways that contribute to diabetic neuropathy. To accomplish this, we have investigated the curcumin derivative J147.

Curcumin is a polyphenol and the active component of turmeric and ginger. These spices have a long history of use in traditional medicine and the use of curcumin as a therapeutic has been investigated in multiple clinical studies against many diseases (Ara et al., 2016). Curcumin has anti-inflammatory, anti-oxidant, and neuroprotective properties, which are all potential contributors to the pathogenesis of diabetic neuropathy (Calcutt et al., 2009). Previous studies have shown that curcumin is effective in treating hyperalgesia, large fiber conduction slowing and central nervous system dysfunction in rodent models of diabetes (Ho et al., 2016; Joshi et al., 2013; Peeyush Kumar et al., 2011; Sharma et al., 2007), making curcumin a plausible therapeutic candidate for diabetic neuropathy. Unfortunately, curcumin demonstrates poor bioavailability and blood brain barrier permeability. To overcome this, we have developed the curcumin derivative J147 using a medicinal chemistry strategy employing cell based phenotypic screening assays based upon aging-associated brain toxicities (Chen et al., 2011). J147 is effective in preventing oxidative stress, reduced mitochondrial function, and nerve cell death due to the loss of trophic support in cell culture models. J147 reverses cognitive impairment in a mouse model of Alzheimer's disease, and enhances memory in both transgenic AD mice, and aged wild type mice. It also reduces inflammation and old age-associated metabolic decline in a mouse model of aging (Currais et al., 2015; Prior et al., 2013) and is neurogenic (Prior et al., 2016). The wide-ranging effects of J147 suggest that it has a strong therapeutic potential to reduce the multiple pathogenic pathways associated with diabetic neuropathy. We have therefore used the STZ induced model of type 1 diabetes in mice to explore the therapeutic effects of J147.

2. Materials and methods

2.1. Protocol

Female Swiss Webster mice were made diabetic by injection of STZ (90 mg/kg intraperitoneal in 0.9% sterile saline) on two consecutive days, with each injection preceded by a 12 h fast, as described in detail elsewhere (Jolivalt et al., 2016). Only animals with blood glucose levels of >15 mM at the start and end of the study were retained as diabetic. HbA1c was measured using the A1CNow kit (Bayer Healthcare, Toronto, Ontario, Canada). Insulin was measured using the ultra-sensitive mouse Insulin ELISA kit. (Crystal Chem). J147 was administered in corn oil vehicle by oral gavage via a gavage needle twice daily starting immediately after confirmation of diabetes.

2.2. Paw thermal sensitivity

Hind paw thermal response was measured as described in detail elsewhere (Jolivalt et al., 2016). Briefly, mice were placed in glass cubicles on top of a modified Hargreaves device (UARD, La Jolla, CA, USA), set at a heating rate of 1 °C/s to selectively activate C fibers (Yeomans and Proudfit, 1996). The heat source was placed directly below the middle of one of the hind paws and the time until paw withdrawal measured. To account for drift in heating rates over time, the apparatus was calibrated daily by constructing a time:-temperature response curve with temperature measured at the lower surface of the glass platform using an inbuilt thermistor. Response latency was converted to response temperature each day by interpolation from the calibration curve (Jolivalt et al., 2016).

2.3. Motor nerve conduction velocity

Motor nerve conduction velocity (MNCV) was measured in mice anesthetized with isoflurane using needle electrodes to stimulate (0.05 ms, 1–5 V) the sciatic nerve at the sciatic notch and Achilles tendon. Evoked electromyograms were recorded using needle electrodes placed in the ipsilateral interosseus muscles and MNCV calculated using the peak-peak latency between pairs of M or H waves and the distance between the two stimulation sites (Jolivalt et al., 2016). Nerve and rectal temperatures were maintained at 37 °C and all measurements were made in triplicate, with the median of the three used to represent values for that animal.

2.4. Paw tactile response threshold

Tactile allodynia was assessed using von Frey filaments as described in detail elsewhere (Jolivalt et al., 2016). Briefly, a series of filaments with a range of buckling forces were sequentially applied to the plantar surface of the mouse hindpaw following the up and down method of Dixon (1980). Data are represented as 50% paw withdrawal threshold (PWT).

2.5. Rotarod

Mice were placed on an accelerating rotarod device (4.0–40.0 rpm in 120 s) and time before falling recorded as described elsewhere (Jolivalt et al., 2016).

2.6. RNA analysis

RNA was isolated from whole brain using the Qiagen RNeasy Plus Universal mini kit (Qiagen). RNA-Seq libraries were prepared using the Illumina TruSeq Stranded mRNA Sample Prep Kit according to the manufacturer's instructions. Gene expression that were differentially expressed between the groups were analyzed using the Ingenuity Pathway Analysis software. (Qiagen).

2.7. Western blots

Tissue samples were homogenized in 10 vol of RIPA lysis buffer (50 mm Tris, pH 7.5, 150 mm NaCl, 0.1% sodium dodecyl sulfate, 0.5% deoxycholate, and 1% NP40) containing a cocktail of protease and phosphatase inhibitors. Samples were sonicated (2×10 s) and centrifuged at $10,000g$ for 60 min at 4 °C. Protein concentrations in the cell extracts were determined using the BCA protein assay (Pierce, Rockford, IL, USA). For SDS-PAGE, 20

μg of protein was used. Plasma samples were added directly to sample buffer. All samples were separated using 10 or 12% Criterion XT Precast Bis-Tris Gels (Bio-Rad, Hercules, CA, USA). Proteins were transferred to nitro-cellulose membranes. Membranes were blocked with 5% skim milk in TBS-T (20 mm Tris buffer pH 7.5, 0.5 m NaCl, 0.1% Tween 20) for 1 h at room temperature and incubated overnight at 4 °C in the primary antibody diluted in 5% BSA in TBS/0.05% Tween 20. Primary antibodies used were: TNFα (CST), TSPO (Abcam), iNOS (BD Biosciences), GFAP (Millipore), Actin (CST), total AMPK (CST), phospho-AMPK (CST), and CRP (Sigma-Aldrich). Subsequently, blots were washed in TBS/0.05% Tween 20 and incubated for 1 h at room temperature in horseradish peroxidase-goat anti-rabbit or goat anti-mouse (Bio-Rad) diluted 1/5000 in 5% skim milk in TBS/0.1% Tween 20. After additional washing, protein bands were detected by chemiluminescence using the SuperSignal West Pico Substrate (Pierce). For all antibodies, the same membrane was re-probed for actin except for CRP where amido black was used. Autoradiographs were scanned using a Bio-Rad GS800 scanner. Band density was measured using the manufacturer's software. Proteins were normalized to actin or albumin band density. Phosphoprotein levels were normalized to total protein expression.

2.8. Statistical analyses

Statistical analysis was carried out by one-way ANOVA followed by Tukey-Kramer multiple comparison *post hoc* test. For data that incorporated multiple time points, two-way repeated-measures ANOVA and *post hoc* Tukey corrected t tests were applied. GraphPad Prism 6 was used to perform statistical analyses. All data are represented as group mean ± SEM.

3. Results

3.1. J147 modulates systemic indices of diabetes

The study contained 4 groups: control treated with vehicle (corn oil) throughout the study, control treated with J147 throughout the study, diabetic treated with vehicle throughout the study and diabetic treated with J147 throughout the 20-week study. J147 is a phenyl hydrazide derived from the natural compound curcumin (Fig. 1F). It was chosen from a large library of derivatives based on phenotypic screening assays and bioavailability (Chen et al., 2015; Prior et al., 2013). Each group began the study with 10 animals. One mouse died in each of the vehicle treated diabetic and J147-treated diabetic groups and one mouse in the vehicle treated STZ-injected group was excluded due to absence of hyperglycemia. At the end of the study body weight was similar in all groups (Fig. 1A) and there was no significant difference in rotarod performance between groups (Fig. 1B). J147 had no impact on blood insulin, glucose or HbA1c levels of control mice (Fig. 1C–E). All groups of STZ-diabetic mice displayed the expected decrease in plasma insulin levels and increase in blood glucose and HbA1c, compared to control mice (all $p < 0.01$ vs control). J147 produced a minor, but statistically significant ($p < 0.05$), decrease in both blood glucose and HbA1c levels in mice treated from onset of diabetes when compared to vehicle treated diabetic mice that was accompanied by a non-significant trend for elevated insulin.

3.2. RNAseq pathway analysis

To assay the effect of J147 on global gene expression in the nervous system, RNA transcripts of whole brain lysate from the control, diabetic + Vehicle and diabetic + J147 groups of mice were quantified using RNAseq technology. Genes demonstrating significant differences in transcript levels were selected and analyzed using Ingenuity Pathway Analysis (IPA). Gene data was standardized to the control + vehicle group. Pathway activation was determined by z-score, and significance determined by the ratio of genes modulated to total genes in a pathway. Heatmap analysis demonstrated distinct grouping between the treatments (Fig. 2A). Diabetes induced significant change in 1073 genes in the vehicle treated group, and 1035 genes in the J147 treated group. Treatment with J147 lead to a significant change in 246 genes compared to the vehicle-treated diabetic group (Fig. 2B). Analysis of function using Ingenuity Pathway Analysis showed a consistent effect of J147 treatment to upregulate nervous system development functions compared to the vehicle-treated diabetic group (Fig. 2C). Pathway analysis showed that the TNFR1 and TNFR2, along with the Type I diabetes mellitus signaling pathways were decreased in diabetic mice by J147 treatment. The AMPK, synaptic long term potentiation, and ephrin receptor signaling pathways were all upregulated by J147 treatment in diabetic mice (Fig. 2D). The top functions significantly changed by J147 in diabetic mice were all related to increased neuron growth and function including proliferation, axon growth and long-term potentiation.

3.3. Protein levels of neuroinflammation markers are decreased by J147

To confirm the effects of J147 suggested by the RNAseq data, whole brain homogenates were assayed by Western blotting to quantify proteins associated with inflammation. J147 was without significant effect on tumor necrosis factor alpha (TNFα), translocator protein (TSPO), inducible nitric oxide synthase (iNOS) or glial fibrillary acidic protein (GFAP) protein levels in the brain of control mice (Fig. 3A). The peripheral inflammation marker C-reactive protein was also not significantly changed by J147 treatment (Fig. 3B). Diabetes increased levels of these proteins compared to vehicle treated control mice and treatment of diabetic mice with J147 from the onset of diabetes caused a significant ($p < 0.05$) reduction in the levels of all 4 proteins.

3.4. The AMPK pathway is stimulated by J147

Reduced AMP kinase signaling is thought to be involved in diabetic neuropathy (Calcutt et al., 2017; Roy Chowdhury et al., 2012) and our RNAseq pathway analysis identified the activation of the AMP kinase pathway as a function of J147 treatment (Fig. 2D). Therefore, total and phosphorylated AMP kinase levels were measured by Western blot (Fig. 3C). J147 was without significant effect on the phosphorylation of AMP kinase, as determined by the phospho/total ratio, in control mice compared to the vehicle-treated control group. Diabetes significantly ($p < 0.01$) decreased AMPK phosphorylation compared to vehicle-treated control mice, and treatment with of diabetic mice with J147 significantly attenuated this decrease ($p < 0.05$ vs diabetes + vehicle group).

3.5. Impact of diabetes and J147 on peripheral nerve function

At study end, the sciatic MNCV of large myelinated fibers was significantly ($p < 0.001$) reduced in vehicle-treated diabetic mice compared to vehicle-treated control mice (Fig. 4A). Treating control mice with J147 for the duration of the study was without significant effect on MNCV, whereas diabetic mice treated with J147 from onset of diabetes had MNCV values that were significantly ($p < 0.001$) higher than vehicle-treated diabetic mice and not different from vehicle treated control mice.

Small unmyelinated fiber-mediated thermal nociception was not different between vehicle-treated control and diabetic mice at the end of the study (Fig. 4B). Both control and diabetic mice treated with J147 showed significant (all $p < 0.001$) paw thermal hypoalgesia at the end of the study compared to vehicle-treated control mice.

Paw response threshold to touch by von Frey filaments was measured at monthly intervals, 24 h after the last treatment with vehicle or J147 (Fig. 4C). J147 treatment was without effect in control mice at any time point. Vehicle-treated diabetic mice developed tactile allodynia (reduced response threshold) that was apparent by week 4 of diabetes and remained throughout the study. At study end, diabetic mice treated with J147 from onset of diabetes had paw withdrawal thresholds that were significantly ($p < 0.001$) higher than vehicle-treated treated diabetic mice but remained significantly ($p < 0.001$) lower than vehicle-treated control mice.

3.6. J147 rapidly alleviates tactile allodynia in diabetic mice and rats

To determine whether the anti-allodynic effect of J147 in diabetic mice was an acute response to the dose given 24hr prior to testing, or represented a change of phenotype, otherwise untreated diabetic mice were given a single intraperitoneal injection of J147 (10 or 50 mg/kg) or vehicle and paw response threshold measured before, and at time points after, treatment. Paw response threshold remained constant compared to pre-treatment values in vehicle-treated control mice at 1,2 and 24 h after treatment and also in vehicle-treated diabetic mice at 1,2,4,6 and 24 h after treatment (Fig. 5A). Both doses of J147 produced rapid alleviation of allodynia in diabetic mice that was maximal at 1hr post-treatment and had resolved by 4–6hr post-treatment. When normalized to pre-treatment values, the efficacy of J147 in alleviating tactile allodynia at 1hr post treatment suggested dose-dependency (Fig. 5B).

To determine whether efficacy of J147 against tactile allodynia in STZ-diabetic mice could be achieved by alternative delivery routes, otherwise untreated mice received a single dose of J147 by oral gavage 12 weeks after onset of diabetes. An anti-allodynic efficacy was observed at 50 mg/kg, was maximal at 1hr post-delivery and had resolved by 2–3 h post-delivery (Fig. 5C). Mice treated with 50 mg/kg J147 also underwent rotarod testing over the same time course. No change from pre-treatment values was noted in the rotarod test (Fig. 5C) indicating that the anti-allodynic effect of J147 was not accompanied by general sedation or loss of sensorimotor function. A similar acute and transient anti-allodynic effect of J147 was noted in an opportunistic study of otherwise untreated 6 week STZ-diabetic rats (Fig. 5D).

4. Discussion

Neuropathy is one of the most common complications of diabetes and there is no therapy available. Both impaired insulin signaling and hyperglycemia are primary pathogenic events and multiple downstream pathways involving such diverse mechanisms as protein glycation, loss of trophic support, mitochondrial dysfunction, oxidative stress and inflammation have been identified in preclinical studies as potential sites for therapeutic intervention (Yagihashi, 2016). It is not clear that blocking one of these pathogenic mechanisms alone will be sufficient to treat diabetic neuropathy and there is an increasing interest in polypharmaceutical approaches that intervene against multiple pathways. While polypharmacy has traditionally required multiple drugs, there is also potential for a single agent to impact multiple pathways. For example, past studies have demonstrated that curcumin may prevent the onset of diabetes (Rouse et al., 2014) and can also impact neuropathy independent of glycemic control (Sharma et al., 2007). Curcumin, while showing some promising therapeutic properties, has distribution and bioavailability issues that restrict its development as a clinically-viable therapy (Hu et al., 2015). We have therefore developed the curcumin derivative J147 using a medicinal chemistry approach that improves bioavailability sufficiently to make it a viable oral drug candidate (Chen et al., 2011; Prior et al., 2014). This approach led to J147 having a half life of 2 and a half hours in the brain, a t_{max} of 2 h and a C_{max} of 203 ng/mL after administration of 20 mg/kg in mice (Prior et al., 2013). J147 has previously demonstrated efficacy in multiple mouse models of Alzheimer's disease and associated CNS inflammation, and has neurotrophic properties (Chen et al., 2011; Currais et al., 2015). The potential of J147 to impact multiple pathogenic pathways associated with diabetic neuropathy prompted us to investigate it in a mouse model of type 1 diabetes.

4.1. J147 had mild effects on the diabetic phenotype

Characterization of the systemic effect of J147 showed no impact on whole body physiology in normal Swiss Webster mice. The regime we used to induce type 1 diabetes in Swiss Webster mice, comprising 90 mg/kg STZ given on two consecutive days, produced marked hyperglyemia and insulinopenia without the cachexic weight loss that is seen in more extreme models that are not considered representative of the current insulin-treated human type 1 diabetic population (Jolivalt et al., 2016). Retention of relatively normal growth and weight in our STZ-injected diabetic mice may therefore be due to the retention of detectable insulin levels in the plasma. J147, given from onset of diabetes significantly lowered terminal blood glucose and glycated hemoglobin levels, measures of acute and long-term glycemic status respectively. STZ is toxic to beta cells within the first 24 h after delivery (Eleazu et al., 2013) and J147 was not given until 5 days after STZ, so it is unlikely that J147 impeded the acute diabetogenic properties of STZ. Curcumin has been reported to enhance beta cell function (Hu et al., 2015) and it is plausible that J147 also enhanced the function of residual beta cells. Indeed, plasma insulin levels at death were elevated in J147-treated diabetic mice, albeit not statistically significantly. While the modest reduction in blood glucose levels is unlikely to explain other effects of J147 on indices of diabetic neuropathy, as J147 treated mice remained markedly hyperglycemic, the small increase in plasma insulin may have direct impact on nerve function. Insulin is a growth factor for

peripheral neurons (Fernyhough et al., 1993) and low levels of systemic or locally delivered insulin protect peripheral nerve structure and function in diabetic rodents without altering hyperglycemia (reviewed in Zochodne, 2016). Further studies are required to determine whether J147 enhances insulin secretion by residual pancreatic beta cells and the extent that this contributes to the neuroprotective properties of J147 in diabetic mice.

4.2. RNAseq analysis demonstrates a neurogenic and anti-inflammatory effect of J147

To confirm that J147 was having biological effects on nervous tissue, we performed whole transcriptome analysis utilizing RNA-seq followed by Ingenuity Pathway Analysis (IPA) on cortical tissue. Comparison of RNA expression between the separate groups showed significant differences in multiple pathways between the experimental groups. Using Ingenuity Pathway Analysis (IPA), pathway modulation was assayed based on changes in RNA expression. The disease and function analysis demonstrated that J147 had a positive effect on neuron development and health. IPA showed J147 treatment lead to a decrease in the expression of genes associated with type I diabetes mellitus signaling and TNF receptor 1 and TNF receptor 2 inflammation pathways. Increased TNFα expression has been implicated in diabetic neuropathy (Yamakawa et al., 2011) and is a possible target for limiting nerve damage (Gonzalez-Clemente et al., 2005; Li et al., 2013; Purwata, 2011). J147 also activated molecular pathways that promote neuronal growth and function, such as AMP kinase, ephrin receptor, and long-term potentiation signaling. Ephrin and long term potentiation signaling are related to new synapse formation and neural outgrowth (Cramer and Miko, 2016), while AMPK regulates many aspects of neuronal bioenergics via mitochondrial biogenesis, turnover and function (Jeon, 2016). To further validate this analysis, we measured levels of selected pertinent proteins in the brains of these mice. Increased levels of proteins associated with inflammation (TNFα, iNOS) and gliosis (GFAP, TSPO) were detected in brain of diabetic mice and were reduced by J147. J147 also reversed the increase in plasma CRP levels induced by STZ treatment. CRP is a standard measure of peripheral inflammation and a common marker for diabetes induced inflammation (Linnemann et al., 2006). The data from transcriptome analysis, as validated by Western blotting, support the capacity of J147 to trigger diverse neuroprotective mechanisms and intervene against multiple pathogenic mechanisms associated with diabetic neuropathy.

4.3. J147 improves motor nerve conduction velocity

Diabetic mice were relatively healthy at the end of the study, as there was minimal weight loss and normal sensorimotor function in the rotarod test. Diabetes induced a broad peripheral neuropathy phenotype, as anticipated from many prior studies (Biessels et al., 2014). These indices of neuropathy are not a consequence of acute direct STZ toxicity (Davidson et al., 2009), but develop slowly and are secondary to insulin deficiency and/or hyperglycemia. Most notably, there was progressive slowing of large fiber MNCV that was prevented by J147 when given from the onset of diabetes. Nerve conduction slowing is widely used in the diagnosis and staging of diabetic neuropathy and serves as the primary quantifiable endpoint in clinical trials of drugs to treat this condition (Bril, 2016; Brill et al., 2016). Diverse pathogenic mechanisms have been proposed from preclinical studies including polyol pathway flux, ischemic hypoxia, oxidative stress, inflammation and loss of neurotrophic support (Yagihashi, 2016). Based on effects of J147 in the brains of these

animals, it is plausible that efficacy against MNCV slowing is related to its AMPK enhancing effects. AMPK depletion has been linked to impaired axonal bioenergetic profile in diabetes (Roy Chowdhury et al., 2012). Moreover, the AMPK activator met-formin both protects nerve conduction and diminishes pro-inflammatory markers such as TNFα and plasma CRP in diabetic rats (Hasanvand et al., 2016) and we found similar effects of J147 on these indices of inflammation. While further studies are required to determine the precise neuroprotective mechanisms of J147 in diabetic neuropathy, efficacy of this curcumin derivative against MNCV slowing supports advancement to clinical investigation.

4.4. J147 induces thermal hyperalgesia

There is increasing focus on small fiber neuropathy in diabetes, as this represents an early functional disorder that impacts quality of life (Malik, 2016). Diabetic rodents are widely reported to show impaired behavioral responses to heat, which can progress from a transient thermal hyperalgesia to hypoalgesia with onset of degenerative neuropathy. We were surprised that 20 weeks of diabetes did not alter paw heat sensitivity in our mice, as we have previously reported onset of paw thermal hypoalgesia after a shorter duration of diabetes in this mouse strain (Beiswenger et al., 2008; Jolivalt et al., 2008; Lee-Kubli and Calcutt, 2014). It is possible that normal heat pain perception may reflect the relatively mild catabolic diabetes in the animals used in the work presented here as our prior study used a more severe diabetes induction regime and produced marked weight loss. It is striking that J147 treatment of both control and diabetic mice significantly increased paw thermal response threshold 24 h after the last treatment. This thermal hypoalgesia did not reflect a general sedative effect, as rotarod performance was unaffected by J147 and suggests a fundamental analgesic effect. As J147 readily crosses the blood-brain barrier (Prior et al., 2013), the site of the analgesic mechanism could range from suppression of nociceptor activity to spinal and suprasinal sensory processing.

4.5. Tactile allodynia is prevented by J147

The analgesic effect of J147 against small fiber mediated heat-induced pain extended to alleviation of tactile allodynia in diabetic mice. Tactile allodynia has been attributed to large myelinated fiber dysfunction in diabetic rodents (Khan et al., 2002) and models the touch-evoked pain described by some diabetic patients (Baron and Maier, 1995). We initially measured paw responses to von Frey filaments some 24 h after last treatment and J147 consistently attenuated allodynia in diabetic mice across the 20-week study without altering the response threshold of control mice. Subsequent studies in otherwise untreated diabetic mice and rats demonstrated an acute and transient an anti-allodynic effect of J147 that was not attributable to general sedation. Thus, J147 can both prevent development of allodynia and rapidly alleviate established allodynia, properties that support its continued development to treat neuropathic pain.

4.6. Conclusion

The capacity for both rapid alleviation of allodynia after a single dose combined with the ability to attenuate onset of allodynia and MNCV slowing in diabetic mice, makes J147 a promising candidate for further development as a treatment for both neuropathy and neuropathic pain.

Supplementary Material

Refer to Web version on PubMed Central for supplementary material.

Acknowledgments

References

Ara SA, Mudda JA, Lingappa A, Rao P. Research on curcumin: a metaanalysis of potentially malignant disorders. J Cancer Res Ther. 2016; 12:175–181. [PubMed: 27072233]

Baron R, Maier C. Phantom limb pain: are cutaneous nociceptors and spinothalamic neurons involved in the signaling and maintenance of spontaneous and touch-evoked pain? A case report. Pain. 1995; 60:223–228. [PubMed: 7784108]

Beiswenger KK, Calcutt NA, Mizisin AP. Dissociation of thermal hypoalgesia and epidermal denervation in streptozotocin-diabetic mice. Neurosci Lett. 2008; 442:267–272. [PubMed: 18619518]

Biessels GJ, Bril V, Calcutt NA, Cameron NE, Cotter MA, Dobrowsky R, Feldman EL, Fernyhough P, Jakobsen J, Malik RA, Mizisin AP, Oates PJ, Obrosova IG, Pop-Busui R, Russell JW, Sima AA, Stevens MJ, Schmidt RE, Tesfaye S, Veves A, Vinik AI, Wright DE, Yagihashi S, Yorek MA, Ziegler D, Zochodne DW. Phenotyping animal models of diabetic neuropathy: a consensus statement of the diabetic neuropathy study group of the EASD (Neurodiab). J Peripher Nerv Syst. 2014; 19:77–87. [PubMed: 24934510]

Bril V. The perfect clinical trial. Int Rev Neurobiol. 2016; 127:27–41. [PubMed: 27133143]

Brill MS, Kleele T, Ruschkies L, Wang M, Marahori NA, Reuter MS, Hausrat TJ, Weigand E, Fisher M, Ahles A, Engelhardt S, Bishop DL, Kneussel M, Misgeld T. Branch-specific microtubule destabilization mediates axon branch loss during neuromuscular synapse elimination. Neuron. 2016; 92:845–856. [PubMed: 27773584]

Calcutt NA, Cooper ME, Kern TS, Schmidt AM. Therapies for hyperglycaemia-induced diabetic complications: from animal models to clinical trials. Nat Rev Drug Discov. 2009; 8:417–429. [PubMed: 19404313]

Calcutt NA, Smith DR, Frizzi K, Sabbir MG, Chowdhury SKR, Mixcoatl-Zecuatl T, Saleh A, Muttalib N, Van der Ploeg R, Ochoa J, Gopaul A, Tessler L, Wess J, Jolivalt CG, Fernyhough P. Selective antagonism of muscarinic receptors is neuroprotective in peripheral neuropathy. J Clin Investigation. 2017; 127:608–622.

Chen HY, Xu DP, Tan GL, Cai W, Zhang GX, Cui W, Wang JZ, Long C, Sun YW, Yu P, Tsim KW, Zhang ZJ, Han YF, Wang YQ. A potent multi-functional neuroprotective derivative of tetramethylpyrazine. J Mol Neurosci. 2015; 56:977–987. [PubMed: 25982925]

Chen Q, Prior M, Dargusch R, Roberts A, Riek R, Eichmann C, Chiruta C, Akaishi T, Abe K, Maher P, Schubert D. A novel neurotrophic drug for cognitive enhancement and Alzheimer's disease. PLoS One. 2011; 6:e27865. [PubMed: 22194796]

Cramer KS, Miko IJ. Eph-ephrin Signaling in Nervous System Development. F1000Res. 2016:5.

Currais A, Goldberg J, Farrokhi C, Chang M, Prior M, Dargusch R, Daugherty D, Armando A, Quehenberger O, Maher P, Schubert D. A comprehensive multiomics approach toward understanding the relationship between aging and dementia. Aging (Albany NY). 2015; 7:937–952. [PubMed: 26564964]

Davidson E, Coppey L, Lu B, Arballo V, Calcutt NA, Gerard C, Yorek M. The roles of streptozotocin neurotoxicity and neutral endopeptidase in murine experimental diabetic neuropathy. Exp Diabetes Res. 2009; 2009:431980. [PubMed: 20148083]

Davidson EP, Holmes A, Coppey LJ, Yorek MA. Effect of combination therapy consisting of enalapril, alpha-lipoic acid, and menhaden oil on diabetic neuropathy in a high fat/low dose streptozotocin treated rat. Eur J Pharmacol. 2015; 765:258–267. [PubMed: 26291662]

Dixon WJ. Efficient analysis of experimental observations. Annu Rev Pharmacol Toxicol. 1980; 20:441–462. [PubMed: 7387124]

Eleazu CO, Eleazu KC, Chukwuma S, Essien UN. Review of the mechanism of cell death resulting from streptozotocin challenge in experimental animals, its practical use and potential risk to humans. J Diabetes Metabolic Disord. 2013; 12:60–60.

Fernyhough P, Willars GB, Lindsay RM, Tomlinson DR. Insulin and insulin-like growth factor I enhance regeneration in cultured adult rat sensory neurones. Brain Res. 1993; 607:117–124. [PubMed: 8481790]

Gonzalez-Clemente JM, Mauricio D, Richart C, Broch M, Caixas A, Megia A, Gimenez-Palop O, Simon I, Martinez-Riquelme A, Gimenez-Perez G, Vendrell J. Diabetic neuropathy is associated with activation of the TNF-alpha system in subjects with type 1 diabetes mellitus. Clin Endocrinol (Oxf). 2005:63. [PubMed: 15963063]

Hasanvand A, Amini-khoei H, Hadian MR, Abdollahi A, Tavangar SM, Dehpour AR, Semiei E, Mehr SE. Anti-inflammatory effect of AMPK signaling pathway in rat model of diabetic neuropathy. Inflammopharmacology. 2016; 24:207–219. [PubMed: 27506528]

Ho C, Hsu YC, Lei CC, Mau SC, Shih YH, Lin CL. Curcumin rescues diabetic renal fibrosis by targeting superoxide-mediated wnt signaling pathways. Am J Med Sci. 2016; 351:286–295. [PubMed: 26992258]

Hu S, Maiti P, Ma Q, Zuo X, Jones MR, Cole GM, Frautschy SA. Clinical development of curcumin in neurodegenerative disease. Expert Rev Neurother. 2015; 15:629–637. [PubMed: 26035622]

Jeon SM. Regulation and function of AMPK in physiology and diseases. Exp Mol Med. 2016; 48:e245. [PubMed: 27416781]

Jolivalt CG, Frizzi KE, Guernsey L, Marquez A, Ochoa J, Rodriguez M, Calcutt NA. Peripheral neuropathy in mouse models of diabetes. Curr Protoc Mouse Biol. 2016; 6:223–255. [PubMed: 27584552]

Jolivalt CG, Lee CA, Beiswenger KK, Smith JL, Orlov M, Torrance MA, Masliah E. Defective insulin signaling pathway and increased glycogen synthase kinase-3 activity in the brain of diabetic mice: parallels with Alzheimer's disease and correction by insulin. J Neurosci Res. 2008; 86:3265–3274. [PubMed: 18627032]

Joshi RP, Negi G, Kumar A, Pawar YB, Munjal B, Bansal AK, Sharma SS. SNEDDS curcumin formulation leads to enhanced protection from pain and functional deficits associated with diabetic neuropathy: an insight into its mechanism for neuroprotection. Nanomedicine. 2013; 9:776–785. [PubMed: 23347896]

Khan GM, Chen SR, Pan HL. Role of primary afferent nerves in allodynia caused by diabetic neuropathy in rats. Neuroscience. 2002; 114:291–299. [PubMed: 12204199]

Lee-Kubli CA, Calcutt NA. Painful neuropathy: mechanisms. Handb Clin Neurol. 2014; 126:533–557. [PubMed: 25410243]

Li Y, Zhang Y, Liu DB, Liu HY, Hou WG, Dong YS. Curcumin attenuates diabetic neuropathic pain by downregulating TNF-alpha in a rat model. Int J Med Sci. 2013; 10:377–381. [PubMed: 23471081]

Linnemann B, Voigt W, Nobel W, Janka HU. C-reactive protein is a strong independent predictor of death in type 2 diabetes: association with multiple facets of the metabolic syndrome. Exp Clin Endocrinol Diabetes. 2006; 114:127–134. [PubMed: 16636979]

Malik RA. Wherefore art thou, O treatment for diabetic neuropathy? Int. Rev Neurobiol. 2016; 127:287–317.

Peeyush Kumar T, Antony S, Soman S, Kuruvilla KP, George N, Paulose CS. Role of curcumin in the prevention of cholinergic mediated cortical dysfunctions in streptozotocin-induced diabetic rats. Mol Cell Endocrinol. 2011; 331:1–10. [PubMed: 20637830]

Pop-Busui R, Martin C. Neuropathy in the DCCT/EDIC-what was done then and what we would do better now. Int Rev Neurobiol. 2016; 127:9–25. [PubMed: 27133142]

Prior M, Chiruta C, Currais A, Goldberg J, Ramsey J, Dargusch R, Maher PA, Schubert D. Back to the future with phenotypic screening. ACS Chem Neurosci. 2014; 5:503–513. [PubMed: 24902068]

Prior M, Dargusch R, Ehren JL, Chiruta C, Schubert D. The neurotrophic compound J147 reverses cognitive impairment in aged Alzheimer's disease mice. Alzheimers Res Ther. 2013; 5:25. [PubMed: 23673233]

Prior M, Goldberg J, Chiruta C, Farrokhi C, Kopynets M, Roberts AJ, Schubert D. Selecting for neurogenic potential as an alternative for Alzheimer's disease drug discovery. Alzheimers Dement. 2016; 12:678–686. [PubMed: 27149904]

Purwata TE. High TNF-alpha plasma levels and macrophages iNOS and TNF-alpha expression as risk factors for painful diabetic neuropathy. J Pain Res. 2011; 4:169–175. [PubMed: 21811392]

Rouse M, Younes A, Egan JM. Resveratrol and curcumin enhance pancreatic beta-cell function by inhibiting phosphodiesterase activity. J Endocrinol. 2014; 223:107–117. [PubMed: 25297556]

Roy Chowdhury SK, Smith DR, Saleh A, Schapansky J, Marquez A, Gomes S, Akude E, Morrow D, Calcutt NA, Fernyhough P. Impaired adenosine monophosphate-activated protein kinase signalling in dorsal root ganglia neurons is linked to mitochondrial dysfunction and peripheral neuropathy in diabetes. Brain. 2012; 135:1751–1766. [PubMed: 22561641]

Sharma S, Chopra K, Kulkarni SK. Effect of insulin and its combination with resveratrol or curcumin in attenuation of diabetic neuropathic pain: participation of nitric oxide and TNF-alpha. Phytotherapy Res. 2007; 21:278–283.

Yagihashi S. Glucotoxic mechanisms and related therapeutic approaches. Int Rev Neurobiol. 2016; 127:121–149. [PubMed: 27133148]

Yamakawa I, Kojima H, Terashima T, Katagi M, Oi J, Urabe H, Sanada M, Kawai H, Chan L, Yasuda H, Maegawa H, Kimura H. Inactivation of TNF-alpha ameliorates diabetic neuropathy in mice. Am J Physiol Endocrinol Metab. 2011; 301:E844–E852. [PubMed: 21810933]

Yeomans DC, Proudfit HK. Nociceptive responses to high and low rates of noxious cutaneous heating are mediated by different nociceptors in the rat: electrophysiological evidence. Pain. 1996; 68:141–150. [PubMed: 9252009]

Zochodne DW. Sensory neurodegeneration in diabetes: beyond glucotoxicity. Int Rev Neurobiol. 2016; 127:151–180. [PubMed: 27133149]

Appendix A. Supplementary data

Supplementary data related to this article can be found at https://doi.org/10.1016/j.neuropharm.2017.11.007.
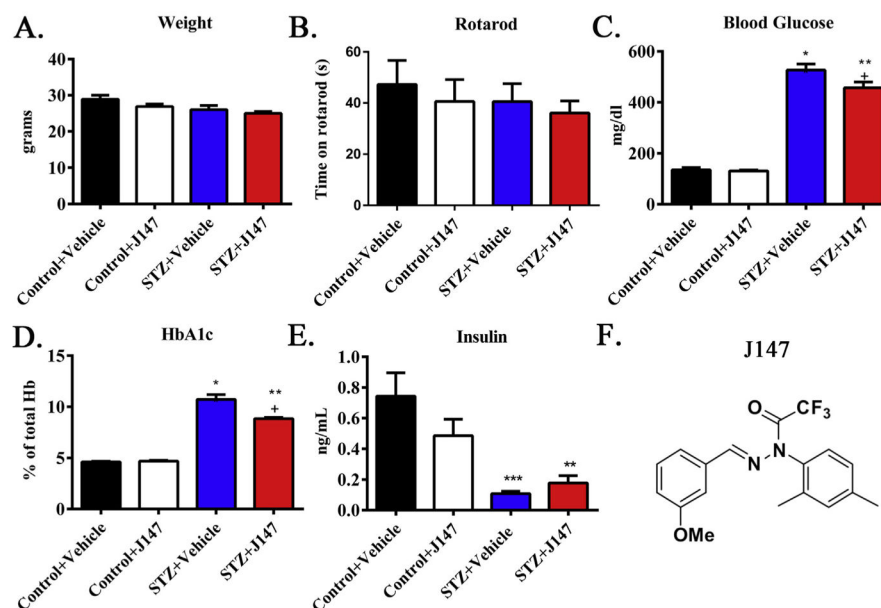
Fig. 1.
Severity of diabetes is modified by J147 treatment. Terminal body weight (A), rotarod performance (B), blood glucose (C), HbA1c (D), and plasma insulin (E) in control mice treated with vehicle (black bars) or J147 (white bars) and STZ-diabetic mice treated with vehicle (blue bars) or J147 (red bars) from onset of diabetes. Chemical structural diagram of J147 (F). Data are group mean + SEM of N = 8–10/group. Statistical analysis by one-way ANOVA with Tukey-Kramer post-hoc test. ** = p < 0.01 versus control + = p < 0.5 vs STZ + Vehicle. (For interpretation of the references to colour in this figure legend, the reader is referred to the web version of this article.)
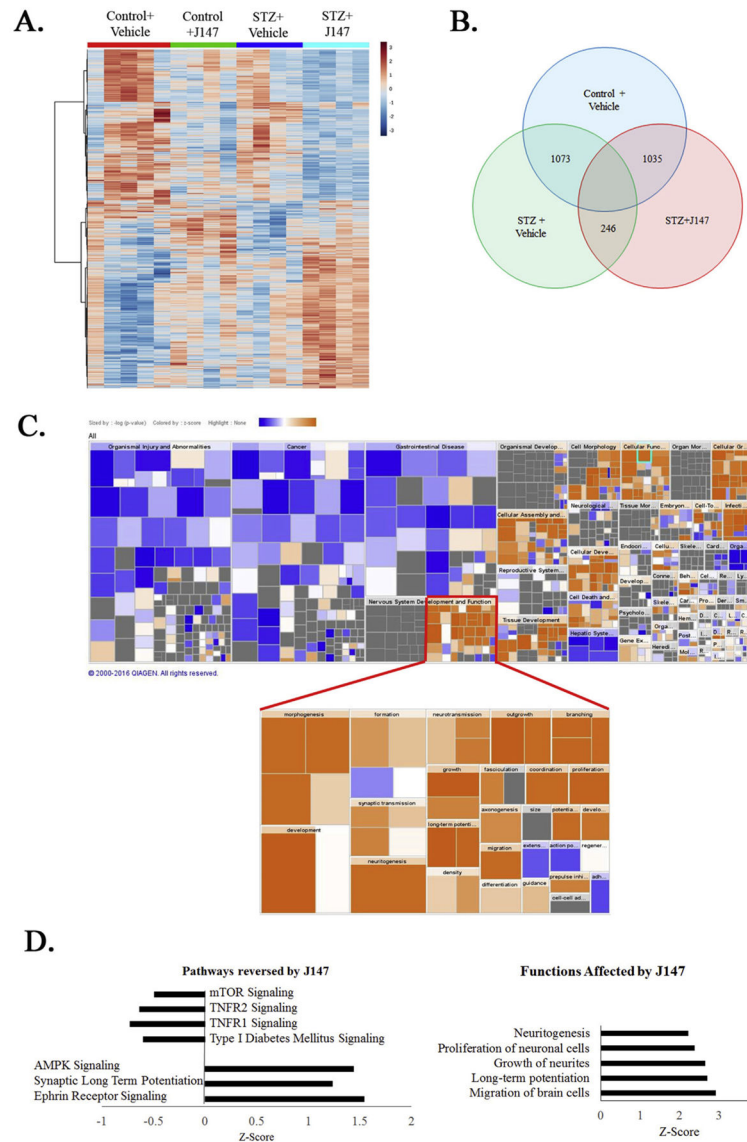
Fig. 2.
RNAseq pathway analysis reveals anti-inflammatory and neurogenic effects of J147. Heatmap of gene expression shows clustering and expression profile of control or diabetic mice treated with vehicle or J147 (A). Total transcriptome analysis compared to the control + vehicle group showed a subset of 246 genes whose diabetes-induced altered expression was altered by J147 treatment (B). Ingenuity pathway analysis demonstrated a strong effect of J147 on nervous system development and function (C). IPA predicted that there was a decrease in TNFα, and diabetes signaling, and an increase in AMPK, synaptic long-term potentiation and ephrin signaling in mice treated with J147. IPA software also predicted induction of neuritogensis, neuron proliferation, neurite growth, migration of brain cells, and long-term potentiation (D).
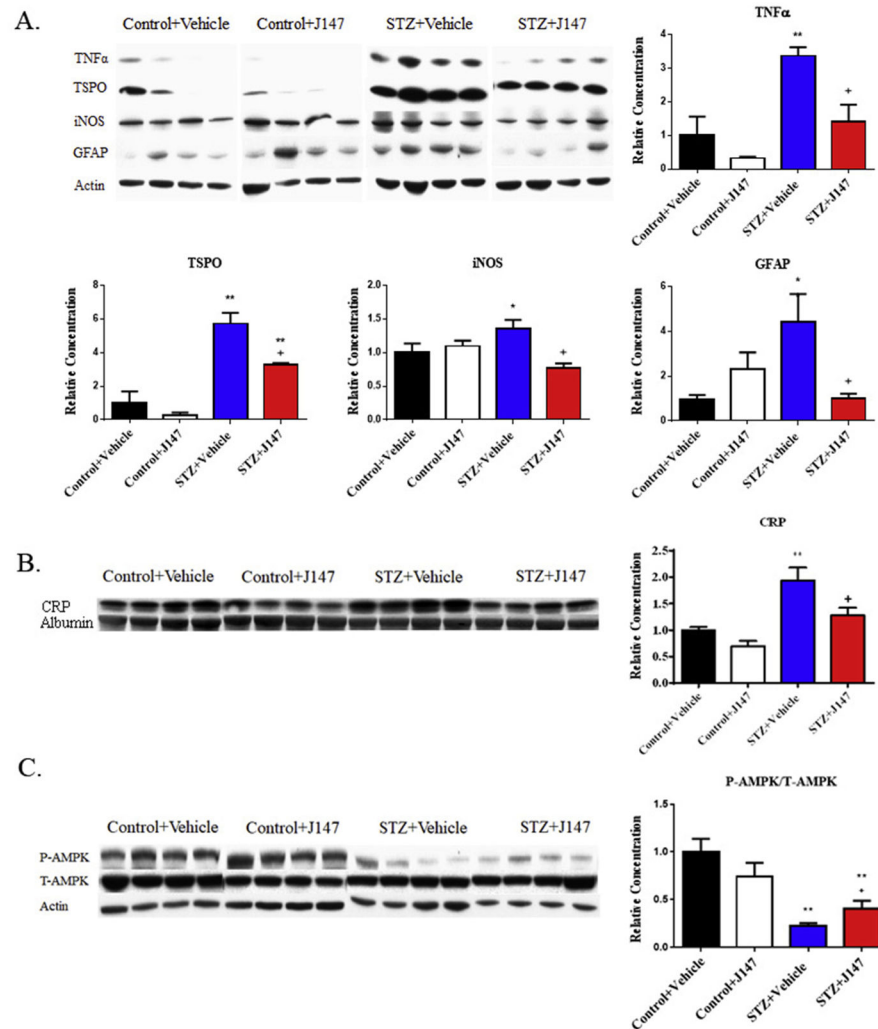
Fig. 3.
Impact of J147 on pro-inflammatory markers and AMPK in diabetic mice. Western blot analysis of whole brain lysates showed a diabetes-induced increase in the protein levels of TNFα, TSPO, iNOS, and GFAP (A) and plasma C-reactive protein (B) that was reduced by J147 treatment. A significant decrease in phosphorylated AMPK in the brain of diabetic mice that was significantly attenuated by J147 (C). Data are group mean + SEM of n = 4/ group. Statistical analysis by one-way ANOVA with Tukey-Kramer post hoc test. * = p < 0.05 vs Control + Vehicle, ** = p < 0.01 vs Control + Vehicle, + = p < 0.05 vs STZ + Vehicle.
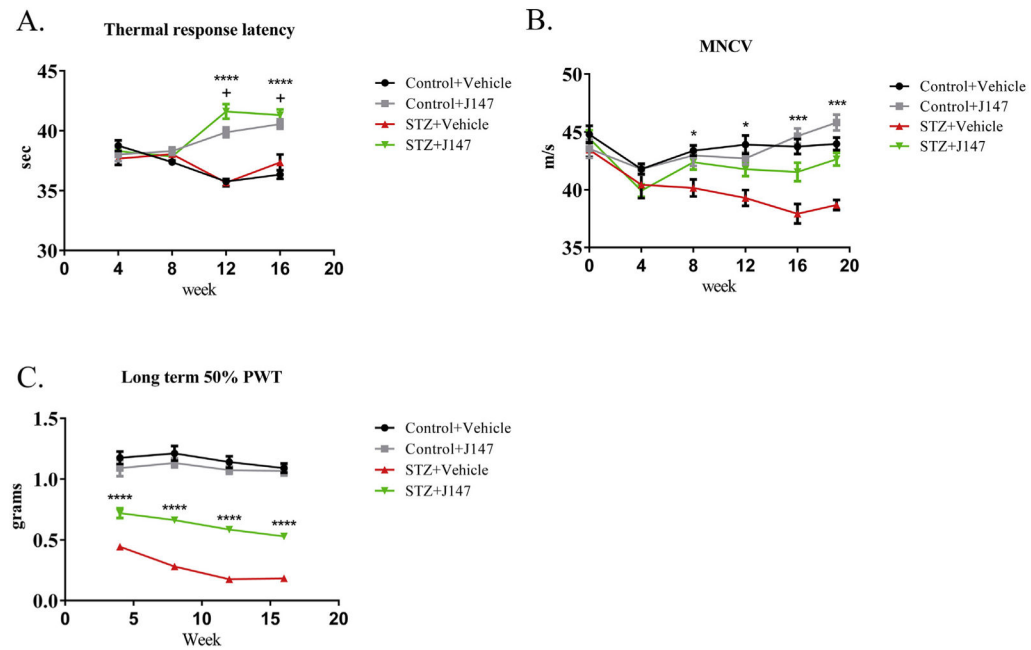
Fig. 4. Impact of J147 on motor and sensory function
Treatment with J147 increased paw thermal response latency of both control and STZ-diabetic mice starting at week 12 (both p < 0.0001 vs STZ + Vehicle or Control + Vehicle respectively) (A). Motor nerve conduction velocity (MNCV) was decreased with progression of diabetes and treatment with J147 rescued this decrease from week 8 onwards (p < 0.05–0.001 vs STZ + Vehicle) (B). Long-term treatment with J147 inhibited the diabetes induced decrease in paw withdrawal threshold (PWT) at weeks 4–16 when measured 24hr after last treatment (all p < 0.0001) (C). Data are group mean + SEM of n = 8/group. Statistical analysis by two-way ANOVA with Tukey's post-hoc test. * = p < 0.05, *** = p < 0.001 and **** = p < 0.0001 for STZ + Vehicle vs STZ + J147, + = p < 0.0001 for Control + Vehicle vs Control + J147 and STZ + J147.
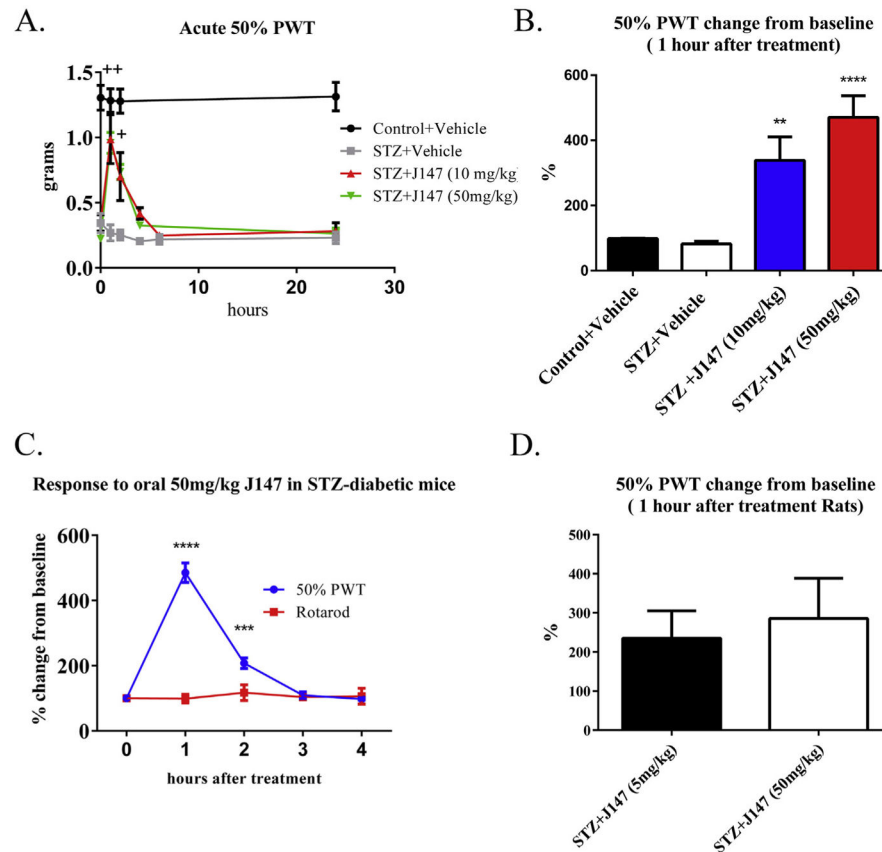
Fig. 5. Impact of J147 on tactile allodynia in diabetes

J147 acutely ameliorated tactile allodynia in both diabetic mice and rats. Acute treatment with J147 (10–50 mg/kg ip) rapidly increased PWT (A), with maximal changes from baseline ($p < 0.01$–0.001) noted 1hr after treatment (B). The change from baseline PWT following 50 mg/kg J147 given orally did not correspond to changes in rotarod performance. (C). J147 treatment also induced a 2-fold change in baseline PWT of STZ-diabetic rats (D). Data are group mean + SEM of n = 7–10/ group. Statistical analysis by two-way ANOVA with Tukey's post-hoc test for A and C; one-way ANOVA with Tukey-Kramer post-hoc test for B and D. * = $p < 0.05$ STZ + Vehicle vs STZ + J147, + = $p < 0.01$ STZ + Vehicle vs STZ + J147 (10 mg/kg and 50 mg/kg), ++ = $p < 0.001$ STZ + Vehicle vs STZ + J147 (10 mg/kg and 50 mg/kg), ** = $p < 0.01$, *** = $p < 0.001$, **** = $p < 0.0001$.